Novel and New Concept to Increase Oxygen Transfer in Bioreactors

Bernat Olle and Daniel I.C. Wang*
Department of Chemical Engineering; Massachusetts Institute of Technology
77 Massachusetts Avenue; Cambridge, MA 02139, USA

*Address all correspondences to Daniel I.C. Wang, Department of Chemical Engineering, MIT, Cambridge, MA 02139; E-mail: <dicwang@mit.edu>

Oxygen transfer enhancement has been observed in the presence of colloidal dispersions of magnetite (Fe_3O_4) nanoparticles coated with oleic acid and a polymerizable surfactant. These fluids improve gas-liquid oxygen mass transfer up to 6 fold (600%) in an agitated, sparged bioreactor and show remarkable stability in high-ionic strength media over a wide pH range. Through a combination of experiments using physical and chemical methods to characterize mass transfer, it is shown that (i) both the mass transfer coefficient (k_L) and the gas-liquid interfacial area (a) are enhanced in the presence of nanoparticles, the latter accounting for a larger fraction of the total enhancement, (ii) the enhancement in k_L measured by physical and chemical methods is similar and ranges from 20% to 60% approximately, (iii) the enhancement in k_L levels off at a nanoparticle fraction mass fraction of approximately 1% v/v.

Introduction

Absorption of gases into a liquid is of crucial importance to multiphase reactions because diffusion of a sparingly soluble gas species across a gas-liquid interface generally limits the reaction rates. This article considers the application of colloidal dispersions of magnetic nanoparticles to mass transfer enhancement in a gas-liquid system. The particle size studied is 3 orders of magnitude smaller than the typical size covered in the previous literature. The dispersions consisted of colloidal aqueous solutions of nanoparticles formed by a core of magnetite (Fe_3O_4) to which a first layer of oleic acid was grafted by chelating bonds to confer high oxygen storage capacity and a second layer of surfactant (Hitenol–BC) was covalently grafted to the first layer to prevent unbounded aggregation.

Nanoparticles have been used for over a decade to increase the heat transfer properties of solutions in a wide range of heat transfer applications; the term *nanofluid* (Choi, 1995) has been coined to describe these dispersions. Research has shown that nanoparticles made of metals, (Eastman et.al, 2001, Patel et.al, 2003, Choi et.al, 2001, Xie et.al., 2003) metal oxides, (Das et.al., 2003, Lee et.al., 1999, Masuda et.al., 1993) and multi-walled carbon nanotubes, Choi et.al., 2001, Xie et.al., 2003) greatly enhance heat transfer in liquids.

Despite the research conducted on nanofluids for heat transfer, the potential application of nanofluids to mass transfer enhancement has thus far been overlooked. Only one

experimental study has been published, (Wen et.al., 2005) where it was reported that nanometer-sized TiO_2 particles reduced the volumetric mass transfer coefficient in a three-phase airlift reactor. In contrast, the present work shows that aqueous solutions of nanoparticles can be used to increase oxygen mass transfer into water by several-fold.

Experimental Methods

Nanoparticle Synthesis and Purification

A solution of 94 g of ferric chloride hexahydrate (97% $FeCl_3 \cdot 6H_2O$, Sigma-Aldrich) and 34.4 g ferrous chloride tetrahydrate (99% $FeCl_2 \cdot 4H_2O$, Sigma-Aldrich) in 100 g of water was stirred at 80 ^oC under nitrogen sparging for 30 min in a round bottom flask. Next, 100 g of potassium oleate (40 wt% paste in water, $CH_3(CH_2)_7CH=CH(CH_2)_7COOK$, Sigma-Aldrich) was added, and the mixture was stirred for an additional 30 min. A 100 mL of an aqueous solution containing 28% ammonium hydroxide (NH_4OH, Mallinckrodt) was added to the mixture, after which the solution immediately turned black because of the formation of magnetite. The reaction continued at 80 ^oC under stirring and nitrogen sparging for 30 min, after which it is assumed that oleic acid had completely coated the magnetite aggregates.

Following the coating of the magnetite aggregates, 100 g of Hitenol–BC (Daiichi Kogyo Seiyaki) and 5 g of ammonium persulfate (>98% $(NH_4)_2S_2O_8$, Sigma-Aldrich) were added to the reaction mixture. The reaction continued at 80 ^oC, under nitrogen sparging and vigorous stirring for 30 min to allow for the formation of covalent bonds between the propenyl group of Hitenol–BC and the double bond in the alkyl chain of the oleic acid. Hitenol–BC is a polyoxyethylene alkylphenyl ether ammonium sulfate that contains a reactive propenyl group; the long PEO chains and the sulfate group confer stability in water when attached to the surface of oleic-acid coated magnetite particles.

The solution was cooled to room temperature and remained in the oven at 80 ^oC overnight, after which most of the residual ammonium hydroxide evaporated. The dispersion was dialyzed against distilled water (14,000 kDa MWCO dialysis membrane, Pals) in a 20 L container under mild stirring for 2 days to remove unreacted potassium oleate, Hitenol–BC, ammonium persulfate, and other salts and metal ions. Finally, the dialyzed solution was kept in the oven overnight at 80 ^oC, after which its solids contents were measured. The final solid contents were typically between 15 to 25% in weight. This synthetic procedure yielded magnetic nanoparticles with an average number diameter between 20 and 25 nanometers (nm).

Determination of the Volumetric Mass Transfer Coefficient (k_La)

Physical Method: Stirred Beaker as Experimental System

Experiments were conducted in a cylindrical, 10.3 cm diameter beaker, filled with 500 mL of liquid, to a liquid height of approximately 6 cm. The liquid was circulated slowly by a 4.5 cm diameter, 4-bladed, axial-flow impeller (pitched-blade with each blade measuring 3 cm wide and 1.5 cm long), placed centrally in the beaker. The free surface of the liquid remained flat, i.e. it did not exhibit a vortex or appear broken at the agitation speeds studied

(300 rpm and 500 rpm). Dissolved oxygen was measured using a dissolved oxygen polarographic sensor (YSI 5010) connected to a data acquisition meter (YSI 5100).
A built-in barometer compensated for slight atmospheric pressure variations between runs. The temperature was regulated at 37±0.5 ^{o}C with a water bath and the pH of the solution was adjusted to 7.0 before the start of the experiment. Oxygen response curves were obtained by first sparging nitrogen until the dissolved oxygen concentration fell to zero and then monitoring the increase in dissolved oxygen concentration due to exposure of the liquid free surface to the room air. To ensure a constant gas-liquid interfacial area (83.3 cm^2), no air sparging was used during the second step. The relatively long duration of the experiments (~1 hour) guaranteed that the time constant of the probe did not affect the response curves. The dissolved oxygen data can be analyzed by constructing a mass balance of oxygen in the liquid phase as follows:

$$\frac{dC_{O_2,bulk}}{dt} = k_L a\left(C^*_{O_2} - C_{O_2,bulk}\right) = k_L aH\left(P^*_{O_2} - P_{O_2,bulk}\right) \quad (1)$$

Where:
k_L is the liquid-side mass transfer coefficient, a is the specific interfacial area, $P_{O2,bulk}$ and P_{O2}^* are the partial pressures of oxygen in the bulk liquid and at saturation, respectively, $C_{O2,bulk}$ and C_{O2}^* are the equivalent liquid phase partial pressure, H is the Henry's law constant at t is the time elapsed.

with $C_{O_2,bulk} = 0$ at t = 0, the integrated form of this expression is:

$$ln\left(1 - \frac{C_{O_2,bulk}}{C^*_{O_2}}\right) = -k_L at \quad (2)$$

Chemical Method: Sodium Sulfite Oxidation

Volumetric Mass Transfer Coefficient ($k_L a$) Determination

Oxygen mass transfer was characterized in a laboratory scale aerated and agitated fermentor using the sodium sulfite oxidation method. In the presence of a Cu^{2+} or Co^{2+} catalyst, sodium sulfite is oxidized according to the following reaction

$$Na_2SO_3 + \frac{1}{2}O_2 \xrightarrow{Cu^{2+}\text{or } Co^{2+}} Na_2SO_4 \quad (3)$$

The reaction rate can be adjusted with temperature or by changing the catalyst concentration so that oxygen transport from the gas to the liquid, rather than the chemical reaction, is the limiting step. The oxygen uptake rate (OUR) is calculated by measuring the effluent gas composition with a mass spectrometer (Perkin Elmer MGA 1600) and performing a mass balance on oxygen of the gas phase through the reactor as follows:

$$OUR = \frac{F_{N_2\,\text{in}}\left[\left(\frac{C_{O_2}}{C_{N_2}}\right)_{\text{in}} - \left(\frac{C_{O_2}}{C_{N_2}}\right)_{\text{out}}\right]}{V} \quad (4)$$

where OUR is the oxygen uptake rate, $F_{N2,in}$ is the flowrate of nitrogen entering the reactor, C_{O2} and C_{N2} are the concentrations of oxygen and nitrogen entering or exiting the reactor, and V is the working volume. The volumetric mass transfer coefficient can then be determined as

$$k_L a = \frac{OUR}{C^*_{O_2} - C_{O_2,\text{bulk}}} \quad (5)$$

where C^*_{O2} is the average liquid phase saturation concentration in equilibrium with the inlet and outlet gas. Experiments were performed in a 20 L (5.5 L working volume) stirred tank reactor (Biolafitte fermentor system, model BL 20.2), equipped with an Ingold type pH electrode, a Biolafitte dissolved oxygen electrode, a temperature probe, a bottom aeration system consisting of a 4-branded rotating sparger, and an agitator with 2 Rushton 4-bladed turbine impellers. A 0.67 M sodium sulfite solution was loaded into the reactor, and then a $1 \cdot 10^{-3}$M solution of copper sulfate catalyst was added. At this catalyst concentration, the mass transfer is not chemically enhanced. The pH was initially adjusted to 8.0 with sulfuric acid to avoid the accelerated reaction regime typical of sodium sulfite solutions at higher pH. Temperature for the experimental runs was maintained at 37±0.5 ^{o}C, except when specified otherwise.

Interfacial Area Determination

Experiments to determine the gas-liquid interfacial area were conducted with the experimental system previously described. The catalyst used was Co^{2+} instead of Cu^{2+} because the former permits operation in a regime where absorption is kinetically enhanced. Interfacial areas can then be calculated from experimental measures of absorption rates.

Results

Mass Transfer Characterization

Physical Method: Mass Transfer in a Stirred Beaker System

The rationale for characterizing mass transfer by a physical method in an agitated beaker is to avoid problems associated with interfacial area and gas holdup. By conducting experiments in a system that has a fixed and known gas-liquid contact area, the results obtained yield information on the value of the mass transfer coefficient, k_L. Oxygen mass transfer into an aqueous liquid phase is enhanced in the presence of nanoparticles, as shown in Figure 1. The time required to reach saturation is reduced by approximately 25% in the presence of a nanoparticle mass fraction of $\phi = 0.005$ (0.05 W/W).

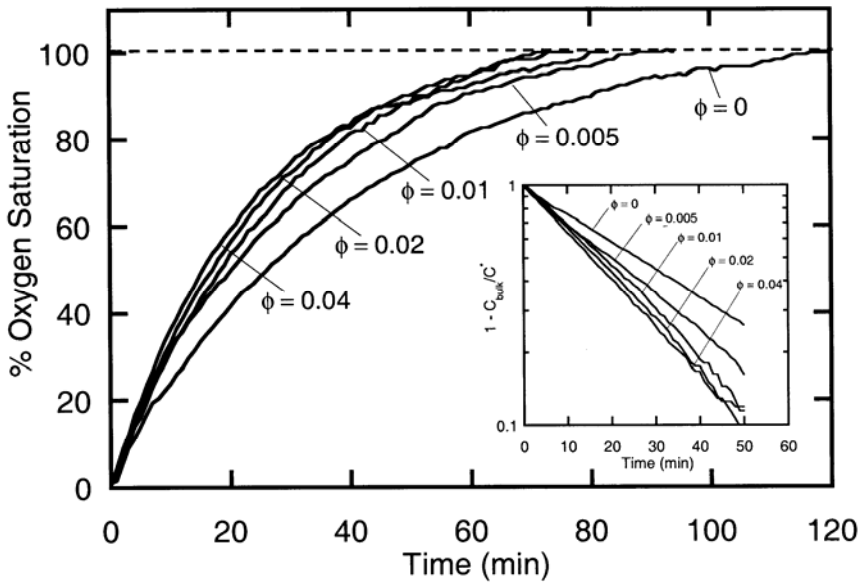

Figure 1: Enhancement of Oxygen Mass Transfer Using Functionalized Magnetic Nanoparticles

Further reductions are attained at larger particle holdups, but the effect is less pronounced above $\phi = 0.01$ (this effect is shown more clearly in Figure 2). The slopes of the first order curves shown in the inset on a semilogarithmic plot in Figure 1 are directly proportional to k_La, and illustrate the increase of k_L in the presence of nanoparticles. The absolute enhancement in k_L, defined as:

$$E = \frac{k_{L,\text{nanoparticles}}}{k_{L,\text{control}}} \tag{6}$$

is plotted in Figure 2 as a function of the nanoparticle holdup for different agitation rates. Data points are the average of 3 experiments. It can be observed that (i) enhancement increases rapidly at low particle holdups and slowly at larger holdups (above $\phi = 0.01$ approximately), and (ii) enhancement is greater at a lower agitation rate because the ratio of k_L values in water at the two agitation speeds studied, $k_{L,500\,rpm} / k_{L,300\,rpm}$, is larger than the equivalent ratio of k_L values in the presence of particles. The value of k_L in water increases by 67% upon changing the agitation speed (from $2.7 \cdot 10^{-5}$ m/s at 300 rpm to $4.5 \cdot 10^{-5}$ m/s at 500 rpm) whereas the value of k_L in the presence of particles increases by a smaller amount at any particle fraction, e.g., by 34% at $\phi = 0.01$.

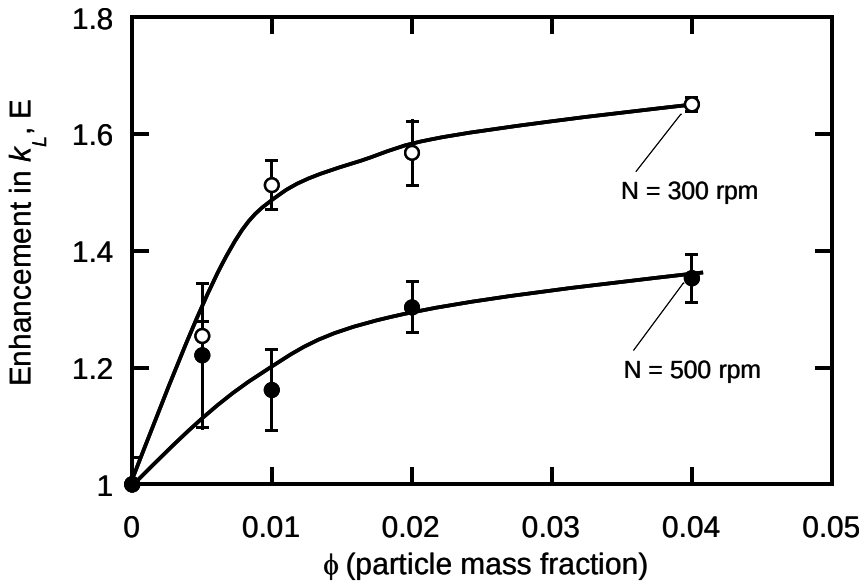

Figure 2: Enhancement of k_L in Surface Aeration at Different Nanoparticle Concentrations

Chemical Method: Sodium Sulfite Oxidation in Bioreactor

This section presents measurements of mass transfer enhancement over a range of values of power input, superficial velocity, and nanoparticle mass fraction obtained using the sodium sulfite method. A convenient feature of this method is that separate determinations of the volumetric mass transfer coefficient k_La and the gas-liquid interfacial area a can be made by manipulating the relative magnitudes of the rate of chemical reaction and the rate of mass transfer.

Determination of the volumetric mass transfer coefficient (k_La)

The absorption flux of oxygen undergoing a pseudo-nth-order reaction with sulfite ions in an aqueous phase can be expressed as :

$$Na = a\left(C^*_{O_2} - C_{O_2,\text{bulk}}\right)\sqrt{\frac{2}{n+1}k_n C^{*\,n-1}_{O_2} D_{O_{2,L}} + k_L^2} \qquad (7)$$

Where:

N is the absorption rate, a is the interfacial area, $D_{O_2,L}$ is the Diffusion coefficient of oxygen in the liquid phase, and n is the reaction order. The relative magnitudes of the rate of oxygen consumption by reaction and the rate of mass transfer can be compared through the Hatta number

$$Ha = \frac{\sqrt{\frac{2}{n+1} k_n C_{O_2}^{*\ n-1} D_{O_{2,L}}}}{k_L} \quad (8)$$

If the following conditions are met, i.e., if

$$C_{O_2,\text{bulk}} = 0 \quad (9a)$$

$$Ha < 0.3 \quad (9b)$$

$$Ha << C_{SO_3^{2-}} / \left(z C_{O_2}^* \right) \quad (9c)$$

where z is a stoichiometric coefficient (moles of sulfite reacted per mole of oxygen), then the reaction is limited by mass transfer and k_La can be obtained from oxygen absorption rates according to:

$$Na = C_{O_2}^* k_L a \quad (10)$$

All of the constraints from Equations 7 through 10 have been shown to have been met. The results are presented in Figures 3 and 4 and showed that a 3 to 4 fold enhancement of k_La can be obtained at a particle mass fraction as low as $\phi = 0.0025$ (0.25% w/v). At higher particle concentrations k_La can still be further enhanced, but diminishing returns are obtained as the particle fraction approaches $\phi = 0.01$. The results illustrate that a several-fold enhancement can be obtained over a broad range of operating conditions of power input per unit volume and superficial velocity.

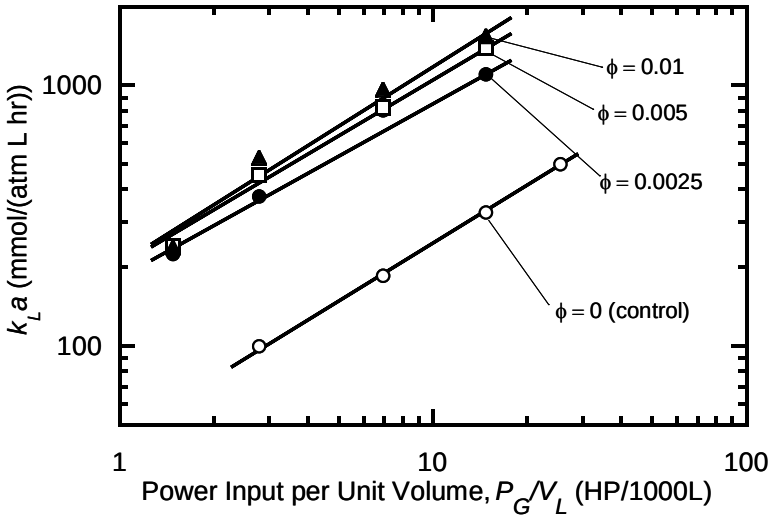

Figure 3: Enhancement of Oxygen Mass Transfer Using Functionalized Magnetic Nanoparticles at Constant Superficial Velocity and Different Nanoparticle Weight Fractions (Φ)

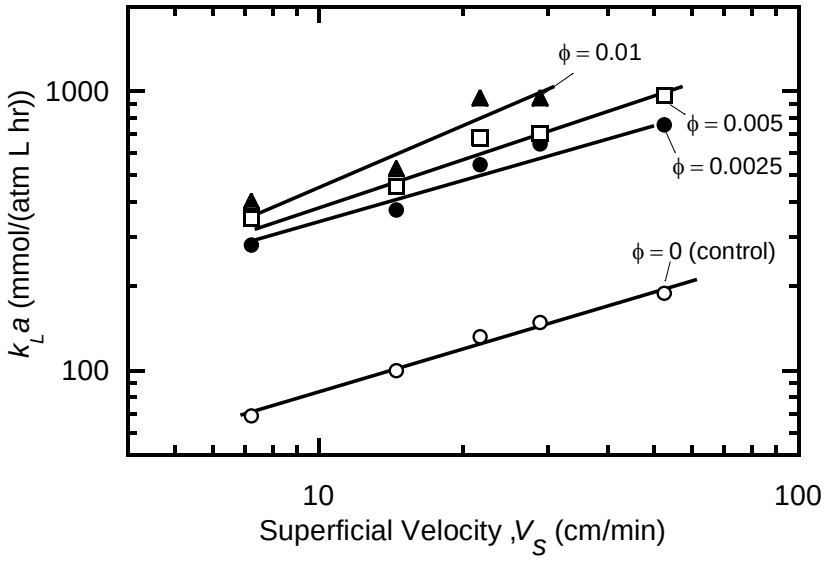

Figure 4: Enhancement of Oxygen Mass Transfer Using Functionalized Magnetic Nanoparticles at Constant Power Per Unit Volume

Figures 5 and 6 show the influence of power input per unit volume and superficial velocity on the absolute enhancement in k_La defined as:

$$E' = \frac{(k_L a)_{\text{nanoparticles}}}{(k_L a)_{\text{control}}} \tag{11}$$

It is apparent from Figure 3 that enhancement initially increases with power input, reaches a maximum, and subsequently decreases. As will be shown in the next section, this trend is caused by the change in interfacial area enhancement as a function of power input. As shown in Figure 6, superficial velocity does not have a noticeable effect on enhancement. Through a non-linear least squares fit of all data presented in Figures 3 and 4, an empirical correlation for k_La as a function of particle mass fraction, power input per unit volume, and superficial velocity is obtained

$$k_L a = 12.9\left(1 + 4.0\phi^{0.34}\right)\left(\frac{P_G}{V_L}\right)^{0.63}(V_S)^{0.57} \tag{12}$$

which, as can be appreciated in Figure 6, gives a satisfactory correlation of all data (P_G/V_L is the gassed power per unit volume and V_S is the superficial gas velocity). This correlation can be used for scale-up purposes but does not contain physical insight into the mechanism of mass transfer enhancement by nanoparticles.

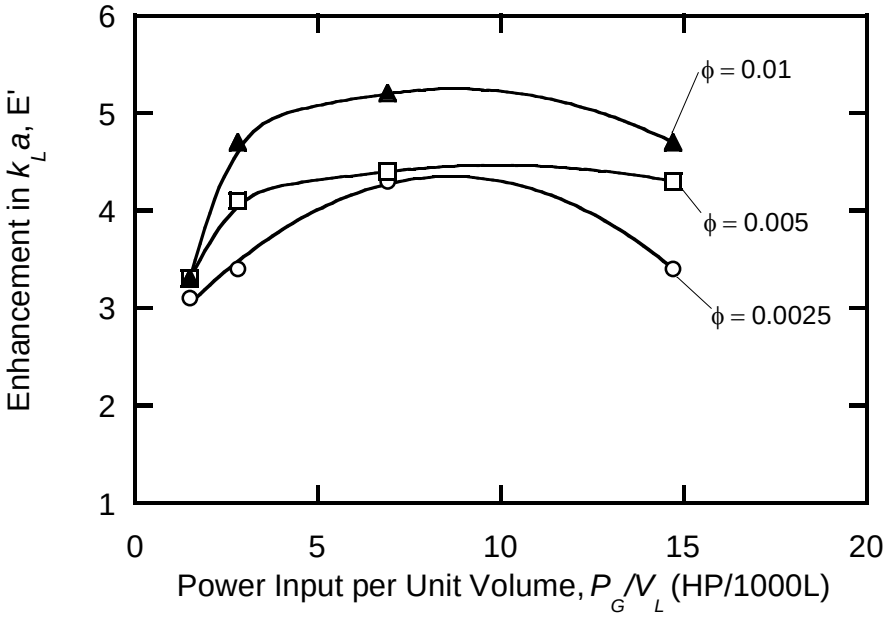

Figure 5: Enhancement of Oxygen Mass Transfer Using Functionalized Magnetic Nanoparticles as Function of Power Per Unit Volume

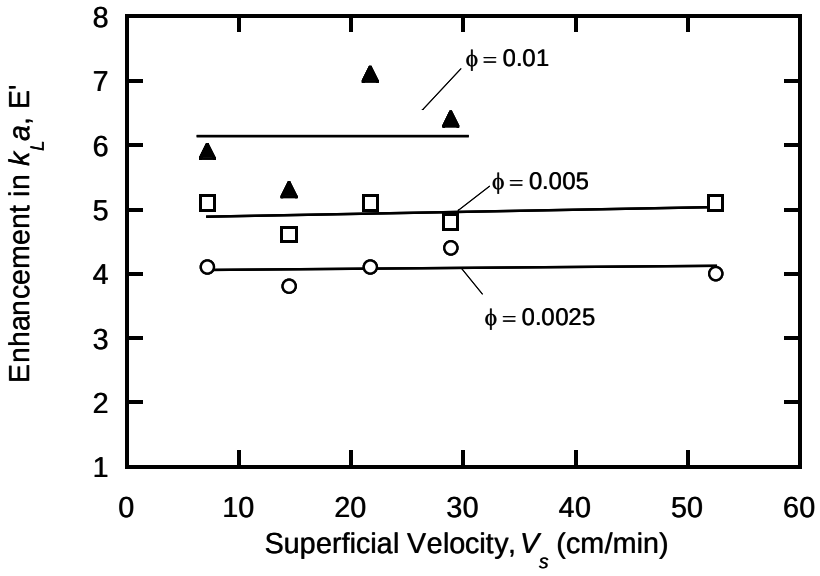

Figure 6: Enhancement of Oxygen Mass Transfer Using Functionalized Magnetic Nanoparticles as Function of Superficial Gas Velocity

Contributions of k_L and Interfacial Area (a) for Mass Transfer Enhancement

From the results on the mass transfer enhancements shown in the pages previously, it would be useful to determine the overall enhancement was the contribution from increased k_L or from the increased interfacial area. It is not possible to provide the underlying principles on which of the two factors contributed to the overall enhancement. It is recommended to the reader that the published paper from our group be examined on the details on what is to be presented (Olle et al, 2006).

From our detailed analyses, the enhancements from k_L and the interfacial area (a) are shown in Figure 7.

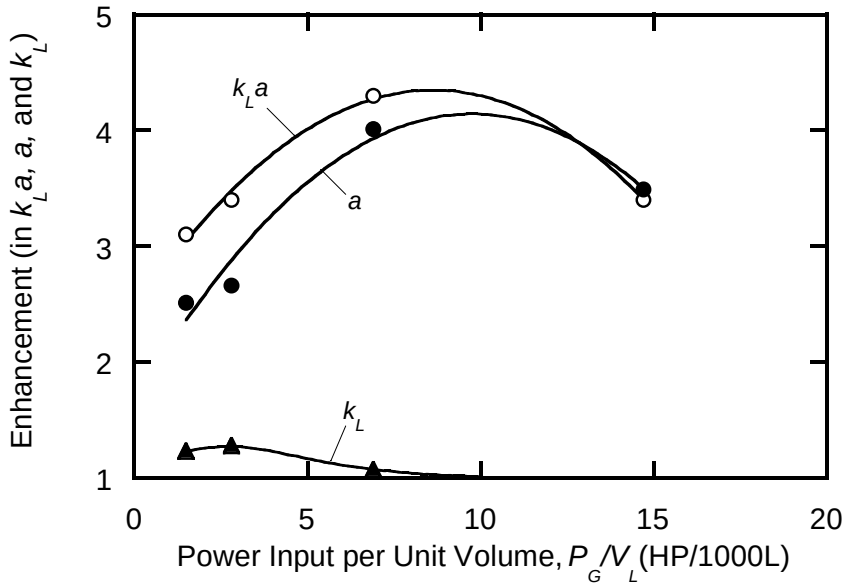

Figure 7: Enhancement of Oxygen Mass Transfer Using Functionalized Magnetic Nanoparticles

The results on the enhancement in Figure 7 were analyzed based on power per unit volume. This was done since it has been shown that increasing superficial gas velocity does not contribute to the overall enhancement. From Figure 7, it is clearly seen that the major contribution to the mass transfer enhancement was the result of increasing the interfacial area (a). More details on the mechanism on this increased interfacial area can be found in the Ph.D. thesis of Olle (2006).

Conclusions

We have presented a new type of dispersion with remarkable stability in high-ionic strength solutions and over a wide range of pH conditions that can be used to enhance gas-liquid oxygen mass transfer up to 6-fold. These findings have direct implications for the field of fermentation. We are currently using nanoparticle dispersions to enhance oxygen uptake rate and cell density in bacterial cultures.

Through a combination of experiments using a stirred beaker system and an agitated, sparged tank we have shown that both the mass transfer coefficient and the interfacial area are enhanced in the presence of nanoparticles, and that the latter accounts for most of the total enhancement. Further, the enhancement in k_L increases rapidly at low nanoparticle holdups and slowly above ϕ=0.01 (approximately). Finally, it has been observed that the enhancement in $k_L a$ shows a strong temperature dependence. Based on these results, our future investigations will attempt to elucidate the mechanism by which nanoparticles increase the gas-liquid interfacial area and the mass transfer coefficient.

Acknowledgement

This work was supported by the DuPont MIT Alliance

References Cited

Choi, S., 1995, *Developments and Applications of Non-Newtonian Flows* pp. 99-105.
Choi, S., Zhang, Z., Yu, W., Lockwood, F., Grulke, E., 2001 *Appl. Phys. Lett.*, 79, (14), 2252-2254.
Das, S., Putra, N., Thiesen, P., Roetzel, W., 2003, *J. Heat Trans-T ASME*, 125, (4), 567-574.
Eastman, J., Choi, S., Li, S., Yu, W., Thompson, L., 2001, *Appl. Phys. Lett.*, 78, (6), 718-720.
Lee, S., Choi, S., Li, S., Eastman, J., 1999, *J. Heat Trans-T ASME*, 121, (2), 280-289.
Masuda, H., Ebata, A., Teramae, K., Hishinuma, N., 1993, *Netsu Bussei (Japan)*, 4, (4), 227-233.
Olle, B., 2006, "Mechanism Modeling of Increased Oxygen Transport Using Functionalized Magnetic Fluids in Bioreactors," Ph.D. Thesis, Department of Chemical Engineering, MIT, Cambridge, MA.
Olle, B., Bucak, S., Holmes, T.C., Bromberg, L., T.A. Hatton and Wang, D.I.C. ,2006, "Enhancement of Oxygen Transfer Using Functionalized Magnetic Nanoparticles," *Industrial Engineering Chemistry Research* 45, 4355-4363.
Patel, H., Das, S., Sundararajan, T., Sreekumaran Nair, A., George, B., Pradeep, T., 2003, *Appl. Phys. Lett.*, 83, (14), 2931-2933.
Wen, J., Jia, X., Feng, W., 2005, *Chem. Eng. Technol.*, 28, (1), 53-60.